

Fast Axial Positioning with Linear-Velocity Control for Linear-Rotary Switched Reluctance Motor

MENG Xuying¹, CAO Xin^{1*}, SHI Ruijie¹, HE Zhouhui¹, DENG Xu², DENG Zhiquan¹

1. College of Automation Engineering, Nanjing University of Aeronautics and Astronautics, Nanjing 210016, P.R. China;
2. School of Engineering, Newcastle University, Newcastle upon Tyne NE1 7RU, U.K.

(Received 16 January 2024; revised 17 April 2024; accepted 10 June 2024)

Abstract: Currently, the axial motion of linear-rotary switched reluctance motor (LRSRM) can only achieve axial positioning, and the two-degree-of-freedom motion is simple. A linear-velocity control method is proposed in the paper to improve the axial control performance. The axial displacement and velocity of rotor are controlled by linear position/velocity observer. The torque winding current and axial-force winding current are calculated by the mathematical model of torque and axial force, and then distributed to the corresponding conducted region for current hysteresis. It can effectively regulate the axial velocity and displacement of the rotor during the rotation process. The effectiveness and accuracy of the proposed method are verified by simulation and experiments.

Key words: multi-degree-of-freedom motor; linear-rotary switched reluctance motor (LRSRM); linear-velocity control; fast axial positioning

CLC number: TM352

Document code: A

Article ID: 1005-1120(2024)03-0300-11

0 Introduction

With the increasing demand for precision of modern industrial drive system, the motor driving and motion control require more dimensions instead of only rotary or linear motion, such as robot arm, multi-coordinate processing, high-grade machine tools, electric gyroscopes and other fields^[1]. However, the traditional motor can only realize rotary motion or linear motion, so it is mostly a single-degree-of-freedom (Single-DoF) motor. In order to meet the urgent requirements of multi-dimensional motion and coordinated control, multiple single-degree-of-freedom motors are often combined through transmission devices, but this method has some shortcomings^[2]: (1) The volume and weight of the system are increased, and there are many parts, large amount of processing and maintenance, and high cost; (2) positioning accuracy and reliability of the system are greatly reduced due to transmission

clearance, wear and aging; (3) the complicated structure of the transmission device increases the moment of inertia and response time of the system, which leads to the deterioration of the dynamic performance of the system. Therefore, it is of great significance to adopt a multi-DoF motor instead of multiple single-DoF motors to improve the accuracy and reliability of the system, reduce the volume and weight of the system, simplify the mechanical structure and reduce the cost.

As a multi-DoF motor, two-DoF linear rotary motor (LRM) can realize rotary, linear and spiral motion without intermediate mechanical conversion mechanism^[3-4]. It greatly improves the mechanical integration and the control accuracy of the system, and has a very broad application prospect in the fields of robot arms and end effectors, aerospace, printed circuit board (PCB) drilling, computerized numerical control (CNC) machine tools, position-

*Corresponding author, E-mail address: caoxin@nuaa.edu.cn.

How to cite this article: MENG Xuying, CAO Xin, SHI Ruijie, et al. Fast axial positioning with linear-velocity control for linear-rotary switched reluctance motor[J]. Transactions of Nanjing University of Aeronautics and Astronautics, 2024, 41(3): 300-310.

<http://dx.doi.org/10.16356/j.1005-1120.2024.03.004>

ing and processing, etc.^[5-7], attracting many institutions and scholars to conduct research in the direction of linear rotary motors. At the same time, some complicated problems that do not exist in the traditional theoretical research of single-DoF motor will be caused due to independent motion of rotation, linear motion and spiral motion composed of them, such as kinematic coupling, electromagnetic coupling, etc.

According to the working principle, LRM can be divided into permanent magnet synchronous motors, reluctance motors and induction motors. Firstly, the induction LRM was proposed to achieve the two-DoF motion in a motor. Later, the permanent-magnet LRMs and reluctance LRMs were proposed and developed, thus the LRMs with different typical motor structures and operational principles have been widely studied.

The linear-rotary switched reluctance motor (LRSRM) combines the switched reluctance motor (SRM) with the linear motor principle, thus it has inherited some advantages of SRMs, i. e. simple structure, no permanent magnets, and flexible control. Sato proposed an LRSRM^[8-9] in 2007. The motor is composed of two stators and a rotor, and the length of the rotor core is less than the total axial length of the two stators. Therefore, if unequal excitations are applied to the windings of the two stators at the same time, the magnetic density at the end of the rotor on both sides will be different, generating thrust to drive the axial movement. An LRSRM composed of three parallel stators and several rotors installed coaxially was proposed in 2011^[10]. Different movements including rotation, linear and combined movements were achieved by applying different winding excitation sequences to the three stators. In Ref.[11], an LRSRM which had two stators connected in series axially was proposed. Each stator had a set of windings. Torque and axial force were generated by controlling the current in the two sets of windings. By controlling the three-phase current of the linear unit winding in different regions, the net torque fluctuated in a small range around 0. The influence on the torque characteristics of the rotational unit can be minimized when the linear unit

winding was conducted, which meant the linear unit would not affect the rotational unit. However, when the rotational unit winding was conducted, it still affected the linear unit. Therefore, appropriate torque and thrust distribution equations were established in Ref.[12], realizing the independent position control of two degrees of freedom. However, this method was difficult to be used in the high-precision position tracking of the LRSRM. To solve this problem, an LRSRM with decoupled structure was investigated^[13-14]. There was no electromagnetic interference between two degrees of freedom. Thus, linear and rotary movement can be controlled independently. However, the axial velocity of the rotor still cannot be adjusted in its control method.

Ref.[15] proposed an LRSRM with a radial double-winding structure, in which the torque winding was mounted across the two stators to provide the main magnetic field, and the axial-force winding provided the bias magnetic field. When the two sets of windings were conducted simultaneously, the magnetic fields under the two stators were different, thus generating an unbalanced magnetic force for axial movement. Afterwards, the mathematical model of torque and axial force was established, and the torque winding current and axial-force winding current were solved to realize the coordinated control of rotational speed and axial position.

Based on Ref.[15], a control strategy that can realize active control of axial velocity is proposed in this paper, which can improve the axial positioning performance. In this paper, the working characteristics and operating principle of LRSRM with two radial windings are analyzed, and a control strategy that can realize active control of axial velocity is proposed, which can improve the axial positioning performance. The rest of the paper is organized as follows. Section 1 shows the structure and motion principle of the LRSRM. The mathematical model of the motor is briefly described in Section 2. Then, in Section 3, the linear-velocity control method is explained. The simulation and experimental results are shown and analyzed in Section 4. Finally, Section 5 draws the conclusions.

1 Topology and Motion Principle of LRSRM

Fig.1 shows the studied LRSRM, which is composed of two stators and one rotor. The two stators are installed in parallel, and two sets of windings are mounted on each stator teeth. As shown in Fig.2, one winding is torque winding, which is mounted across the two stators; the other winding is axial-force winding, which is mounted in the two-stator teeth respectively, and then connected in opposing direction. The torque winding mainly provides the main magnetic flux to generate the torque needed by rotation, and the axial-force winding mainly provides unbalanced magnetic flux to generate the axial force needed by linear motion.

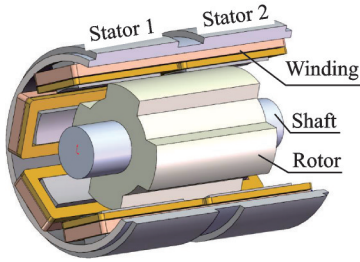


Fig.1 LRSRM structure

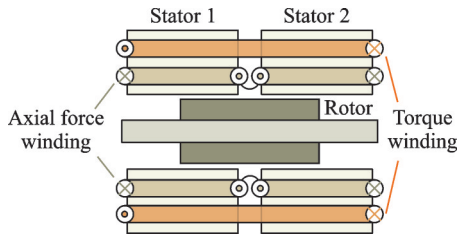


Fig.2 Winding configuration

In the studied LRSRM, the torque winding is conducted unidirectionally and the axial-force winding is conducted bidirectionally. Therefore, the magnetic-flux density increases at one end and decreases at the other end, resulting in unbalanced electromagnetic force. As shown in Fig.2, the magnetic-flux density by the two stator windings increases at the end of Stator 2, and decreases at the end of Stator 1. Therefore, the unbalanced electromagnetic force generated between the two stators can pull the rotor from Stator 1 to Stator 2 along the axial direction.

Therefore, the direction of the generated unbalanced electromagnetic force can be regulated by changing the direction of the axial-force winding current. In addition, the principle of rotation of LRSRM is similar to that of traditional SRMs.

2 Mathematical Model

Before deriving the mathematical model, the following assumptions are made:

- (1) Ignore leakage flux at the end.
- (2) The rotor rotates counterclockwise for positive.
- (3) Ignore the air-gap permeance between two stator teeth.

The air-gap permeance is calculated by dividing it into parts. When the rotor tooth pole axis coincides with the stator tooth pole axis, the rotor position angle is zero.

The specific derivation of magnetic co-energy is shown in Ref.[15]. The expression is as

$$W' = \frac{1}{2} \begin{bmatrix} i_{ta} & i_{fa} \end{bmatrix} L_1 \begin{bmatrix} i_{ta} \\ i_{fa} \end{bmatrix} = \frac{1}{2} L_{ta} i_{ta}^2 + M_{tafa} i_{ta} i_{fa} + \frac{1}{2} L_{fa} i_{fa}^2 \quad (1)$$

where i_{ta} and i_{fa} are the torque-winding current and the axial-force winding current, respectively. L_1 is the winding inductance matrix of phase A, which can be derived by equivalent magnetic circuit diagrams of the two stators and the flux continuity theorem. L_{ta} and L_{fa} represent the self-inductance of torque winding and the self-inductance of axial-force winding, respectively. M_{tafa} is the mutual inductances of two sets of windings.

Torque T and axial force F are obtained by differentiating rotor position angle and axial displacement by air gap magnetic co-energy, respectively. When θ is at $(-30^\circ, 0^\circ)$, we have

$$\begin{cases} T = K_{t1} (N_t^2 i_{ta}^2 + N_f^2 i_{fa}^2) + K_{t2} N_t N_f i_{ta} i_{fa} \\ F = K_f N_t N_f i_{ta} i_{fa} \end{cases} \quad (2)$$

where K_{t1} is the torque coefficient, K_{t2} the function of axial displacement and rotor position angle θ , K_f the axial-force coefficient, N_t the number of turns of torque winding of single tooth pole, and N_f the num-

ber of turns of axial-force winding of single tooth pole. The coefficient expression is

$$\begin{cases} K_f = \left[\frac{\mu_0 r \left(\frac{\pi}{6} + \theta \right)}{l_g} + \frac{4\mu_0}{\pi} \ln \left(\frac{\pi l_g - 4cr\theta}{\pi l_g} \right) \right] \\ K_{t1} = \left[\frac{\mu_0 r (h_r - \delta)}{4l_g} - \frac{\mu_0 (h_r - \delta)}{\pi} \frac{4cr}{\pi l_g - 4cr\theta} \right] \\ K_{t2} = x \left[\frac{\mu_0 r}{l_g} - \frac{4\mu_0}{\pi} \frac{4cr}{\pi l_g - 4cr\theta} \right] \end{cases} \quad (3)$$

where r is the radius of the rotor, h_r the axial length of the rotor, l_g the length of one-sided air gap, μ_0 the air permeability, and $c=1.49$.

3 Linear-Velocity Control Method

3.1 Principle of current control method

Fig.3 shows the inductance curve of the three-phase winding of the motor and the current conducting interval of LRSRM. T_A , T_B and T_C represent the torque winding conduction intervals of phases A, B and C, respectively. F_A , F_B and F_C represent the axial-force winding conduction intervals of phases A, B and C, respectively.

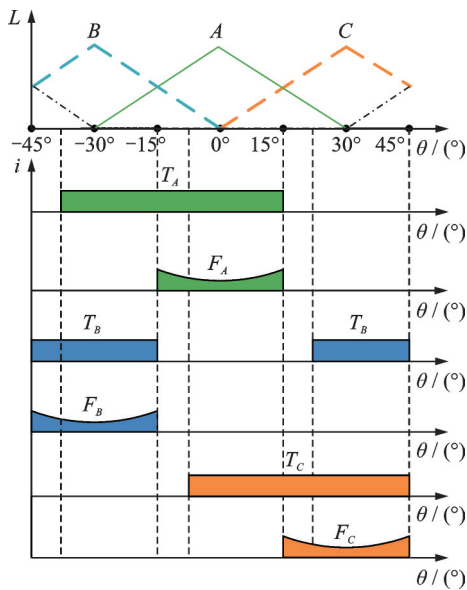


Fig.3 Current conducting interval of LRSRM

The horizontal axis is the rotor position angle θ . Define $\theta = 0^\circ$ where the tooth pole axes of stator and rotor coincide. Taking phase A as an example,

the winding current conducting interval is divided into two parts. One is the axial-force region and the other is the torque region. As shown in Fig.3, the inductance of phase A rises in the range of -30° to 0° , which means positive torque is generated. In the range of -15° to 15° , the inductance of phase A is large. Therefore, the axial force is large, and since the inductance of phase A is symmetrical about 0° , its total torque from -15° to 15° is 0. Therefore, -15° to 15° is called the axial-force region of phase A winding, and -30° to -15° is called the torque region.

According to the principle of magnetomotive force balance, when the magnetomotive force of the torque winding and the axial-force winding are equal, the axial force is the largest and the torque is the smallest. Therefore, the magnetomotive force of the two sets of windings can be made the same in the axial-force region, and the given values of the two sets of windings are calculated accordingly.

Taking phase A as an example, the mathematical expression is

$$\begin{cases} i_{ta} = \frac{\sqrt{F_x/K_f}}{N_t} \\ i_{fa} = \frac{\sqrt{F_x/K_f}}{N_f} \end{cases} \quad (4)$$

where i_{ta} represents the given value of phase A torque-winding current, i_{fa} the given value of phase A axial-force winding current, and F_x the axial force.

3.2 Proposed linear velocity control

The control block diagram of the whole system is shown in Fig.4. Based on the independent control strategy^[15], the proposed control method can achieve fast axial positioning through the active regulating of the linear velocity. In Fig.4, v_{ref} is the given linear velocity, v the actual linear velocity, F_z^* the given value of the axial force, i_f the actual axial-force winding current, i_f^* the given value of the axial-force winding current, i_t the actual torque-winding current, i_{t1}^* the given torque-winding current in the torque region, and i_{t2}^* the given torque-winding cur-

rent in the axial-force region. Table 1 shows the linear position/velocity observer, where z^* represents the reference displacement, z the actual axial displacement, v^* the initial reference value of axial velocity, and v_{ref} the given linear velocity after passing the linear position/velocity observer.

Table 1 Linear position / velocity observer

Displacement relationship	Given linear velocity
$z^* - z > 0$	$v_{ref} = v^*$
$z^* - z = 0$	$v_{ref} = 0$
$z^* - z < 0$	$v_{ref} = -v^*$

The linear position/velocity observer determines the relationship between the real-time axial position and the reference displacement of the rotor, and then sets the magnitude and direction of linear velocity. The rotor can move to the targeted axial position with the given axial velocity, so that the axial positioning time can be adjusted.

The upper part of Fig.4 shows the linear-velocity control loop. Firstly, through the linear position/velocity observer, the given linear velocity is selected. Then actual displacement detected by the axial position sensor is differentiated to obtain the actual linear velocity of the rotor. Through the closed loop of linear velocity, the given value of the axial force obtained by PID controller is sent to the axial-force model calculation module together with the detected rotor position angle. From the equal magnetomotive force of the two sets of windings in the axial-force region, the given currents of the two sets of wind-

ings in the axial-force region, i_{t1}^* and i_{t2}^* , can be obtained. i_t^* is the given value of the axial-force winding current, and it passes through hysteresis cycle with the actual axial-force winding current to generate the control signal required by the power converter connected with the axial-force winding, thus realizing the inner current loop.

The lower part of Fig.4 is the control block diagram of rotary motion. The difference between the given speed and the actual speed is adjusted by the PI controller to obtain the given torque-winding current i_{t1}^* in the torque region. The given torque-winding current is selected between i_{t1}^* and i_{t2}^* according to rotor position angel θ , and then i_t passes through hysteresis cycle with the actual torque-winding current to generate the control signal required by the power converter connected to the torque winding.

3.3 Main circuit topology

Axial force of the LRSRM is generated by the unbalanced magnetic field formed by the simultaneous conduction of torque winding and axial-force winding. In order to facilitate the control of direction of axial force, the direction of torque-winding current is fixed. The direction of axial force can be changed by changing the direction of the axial-force winding current.

The torque winding adopts an asymmetric half-bridge power circuit, as shown in Fig.5. A, B and C represent the three-phase torque winding, T_1-T_6 are the three-phase MOSFET, and D_1-D_6 represent the three-phase power diodes.

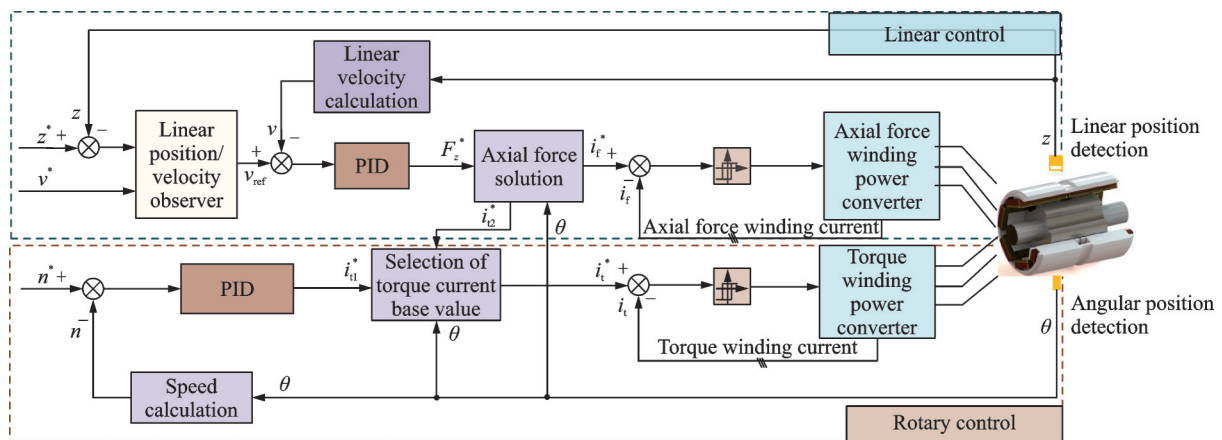


Fig.4 Control block diagram of proposed LRSRM

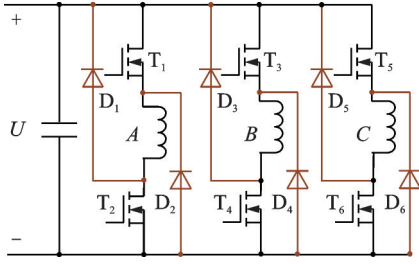


Fig.5 Torque winding power converter

The axial-force winding adopts a three-phase four-bridge-arm topology circuit, as shown in Fig.6, which can reduce the number of switching tubes and satisfy the requirement of bi-directional current flow in the axial-force winding.

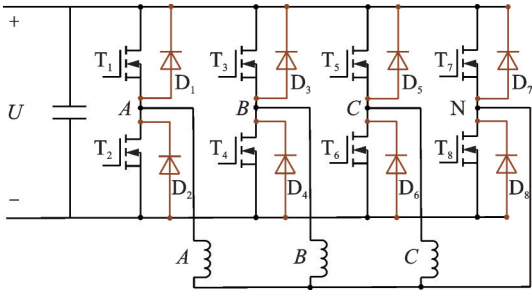


Fig.6 Axial-force winding power converter

4 Simulation and Experimental Results

4.1 Simulation results

Based on MATLAB/Simulink platform, the simulation model of LRSRM linear-velocity control is built to verify the effectiveness of the proposed method. The parameters are listed in Table 2.

Table 2 Experimental parameters

Parameter	Value
Bus voltage/ V	10
Rotor mass/ kg	4
Linear motion stroke/ mm	± 20
Rotational speed/($r \cdot \text{min}^{-1}$)	200
Torque-windings N_t /($\text{turn} \cdot \text{phase}^{-1}$)	38
Axial-force windings N_l /($\text{turn} \cdot \text{phase}^{-1}$)	40
Inside diameter of rotor r / mm	27
Axial length of stator pole/ mm	87
Outside diameter of stator pole/ mm	155
Inside diameter of stator pole/ mm	66.8
Thickness of stator core/ mm	11.2

Fig.7 shows the flow chart of the proposed linear-velocity control method which is employed to control the LRSRM, realizing the active control of axial and rotational directions and adjustable axial positioning velocity.

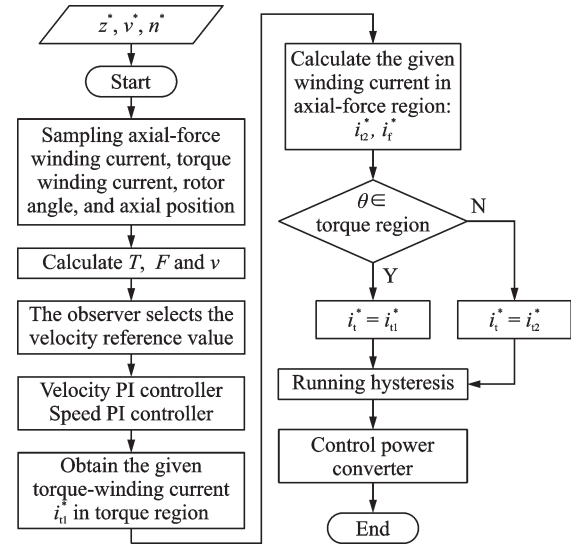


Fig.7 Flow chart of the control method

Fig.8 is the dynamic simulation result of the sudden change of the given linear velocity. When $t=1$ s, the given linear velocity suddenly changes from 0.02 m/s to 0.04 m/s. Fig.8(a) shows the waveform of linear velocity. It can be seen that the response speed is very fast, and the axial velocity is stable at the given value of 0.02 m/s and 0.04 m/s. Fig.8(b) shows waveform of axial force. When $t=1$ s, the axial force obviously increases to about 5 N, and then quickly decreases to 3 N. Fig.8 shows the axial-force winding currents of the three phases: phase A (yellow curve), phase B (orange

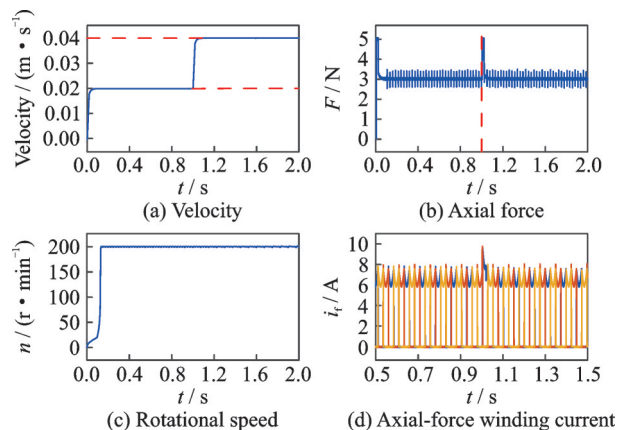


Fig.8 Simulation results of linear velocity changing from 0.02 m/s to 0.04 m/s

curve) and phase C (blue curve). The axial-force winding current obviously increases to 9.5 A when $t=1$ s, and then rapidly decreases to the steady-state value, which is consistent with the change of axial force. Fig.8(c) shows that when the axial velocity suddenly changes, the rotational speed is still stable at 200 r/min, and the fluctuation range is within 1%.

Fig.9 shows simulation results when the given axial position is abruptly changed from 0.02 m to 0.04 m when $t=1$ s. Fig.9(a) shows the dynamic process where the rotor starts to move axially. Fig.9(b) shows that the rotor moves to the given axial position at given velocity of 0.04 m/s, and then the linear velocity drops to 0 in 0.06 s. When the given axial position is abruptly changed, the linear velocity quickly rises to the given velocity of 0.04 m/s within 0.1 s. The axial-force waveform is shown in Fig.9(d). When the axial movement of rotor stops, the axial force instantly drops to the amplitude-limiting value of -5 N, and stabilizes again at 3 N in 0.01 s. When the axial movement of rotor starts, the axial force instantly rises to the amplitude-limiting value of 5 N, and then returns to steady-state value of 3 N in 0.07 s. Fig.9(c) shows the waveform of rotational speed. It is still stable at 200 r/min, and the fluctuation range is within 1%.

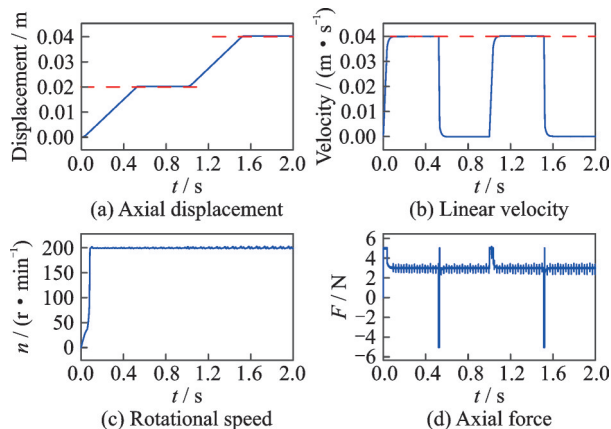


Fig.9 Simulation results of axial position changing from 0.02 m to 0.04 m

There is no overshoot in the linear velocity and the response time is short when the given axial position is changed. The validity of the linear-velocity control method is verified.

4.2 Experimental results

In order to fully verify the effectiveness of the active axial-velocity control algorithm, the DSP digital control platform is built, as shown in Fig.10.

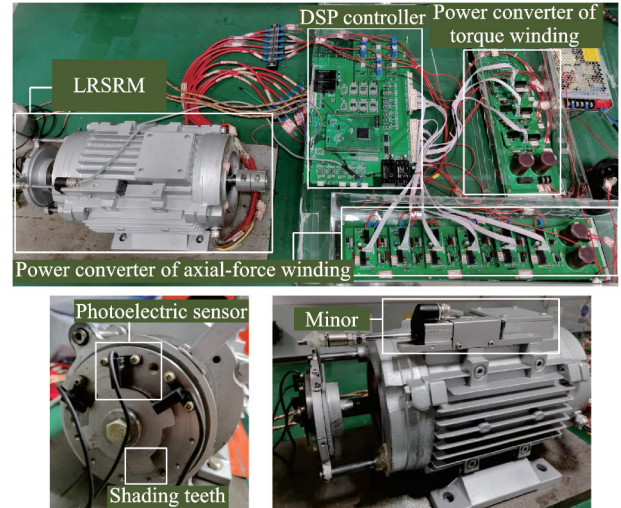
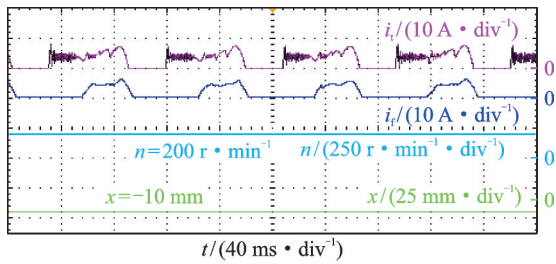


Fig.10 Pictures of experimental platform

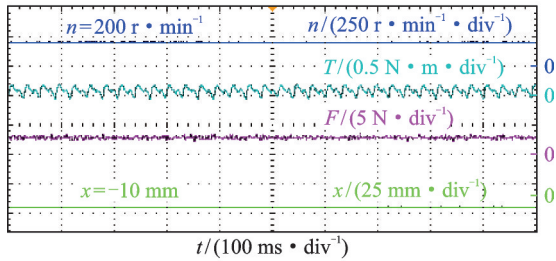
Fig.11 shows the output waveforms of torque-winding current i_{at} , axial-force winding current i_{af} , rotary speed n and axial displacement x when the rotor is controlled to keep the axial position unchanged under the axial load of 3 N. The initial axial position of the rotor is -10 mm. The rotary speed is stable at 200 r/min. The torque-winding current is about 8 A, and the axial-force winding current is about 6 A. The waveforms of the torque and axial force are shown in Fig.11(b).

Fig.12 shows the dynamic experimental results using the linear displacement control method proposed in Ref.[15]. The rotor rotates at 200 r/min. The axial position of the rotor is set from -10 mm to 10 mm in Fig.12(a). In this control method, it takes about 1.5 s to move axially from -10 mm to 10 mm. The linear velocity is not adjustable. Fig.12(b) shows the experimental results when the rotor reciprocates axially from -10 mm to 10 mm. The regulation time is about 0.8 s which is not adjustable.

Fig.13 shows the dynamic experimental results of linear velocity control. The given linear velocity of rotor is 0.04, 0.06, 0.08, and 0.1 m/s, respectively. The axial displacement of the rotor is set from -10 mm to 10 mm. Compared with Fig.13, i_{at}

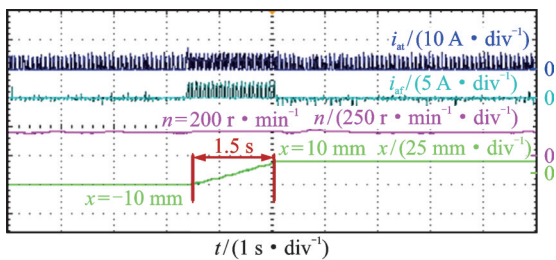


(a) Torque-winding current and axial-force winding current

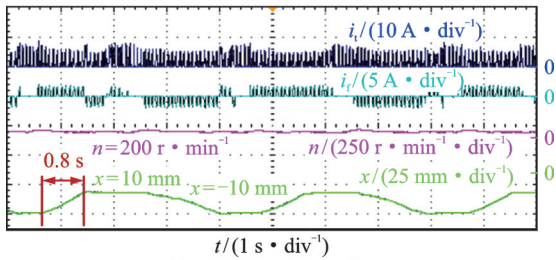


(b) Torque and axial force

Fig.11 Steady experimental results for linear velocity control



(a) Axial position changes (-10 mm to 10 mm)

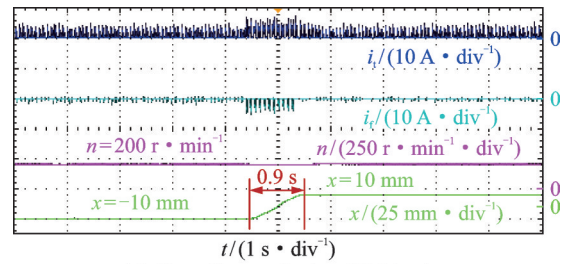


(b) Reciprocating motion

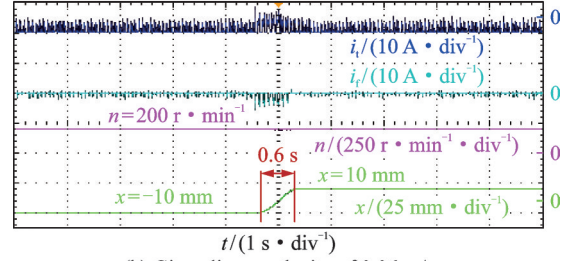
Fig.12 Dynamic experiments of linear displacement control

can be clearly observed that the time taken to run the same axial distance is 0.9, 0.6, 0.4, and 0.3 s, respectively. The validity of the linear-velocity control algorithm is verified. The non-linear relationship is due to the fact that the axial-velocity detection in the experiment is discrete rather than continuous, and in the response process, the axial movement of the rotor has a process of acceleration and deceleration.

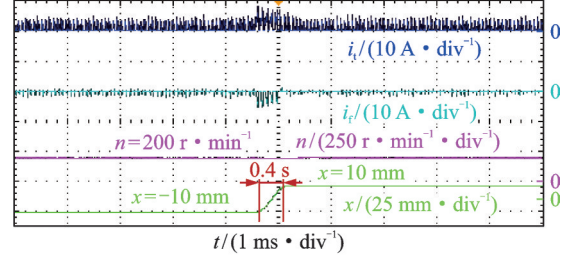
Fig.14 shows the waveform of the axial force of dynamic experiment of linear velocity control.



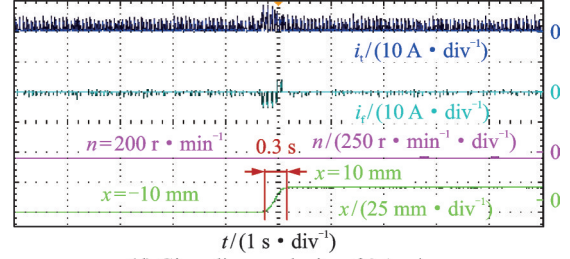
(a) Given linear velocity of 0.04 m/s



(b) Given linear velocity of 0.06 m/s



(c) Given linear velocity of 0.08 m/s



(d) Given linear velocity of 0.1 m/s

Fig.13 Dynamic experiments of linear velocity control

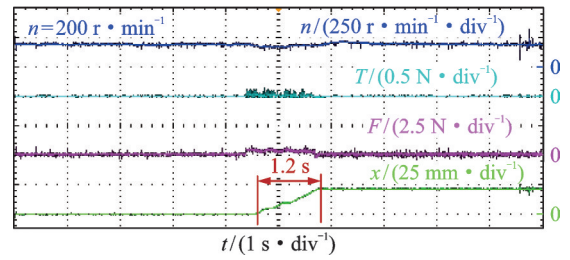


Fig.14 Dynamic experiments of linear velocity control

When the rotor moves axially, the axial force increases to 0.5 N. Since the torque is related to the axial-force winding current, the torque is increased by 0.1 N·m.

Fig.15 shows the waveforms of linear velocity control when the rotor reciprocates under axial no-load condition. The cycle of reciprocating motion is

all set to 4.4 s. Meanwhile, the given linear velocity of rotor is 0.02, 0.03, 0.04, and 0.06 m/s, respectively. In the first half of the cycle, the rotor moves in the positive direction, and the velocity drops to 0 after reaching the given axial position. In the second half of the cycle, the rotor moves in the opposite direction, and the velocity drops to 0 after returning to the initial axial position. It can be seen that during the reciprocating movement of the rotor, its rotary speed is still basically stable at 200 r/min.

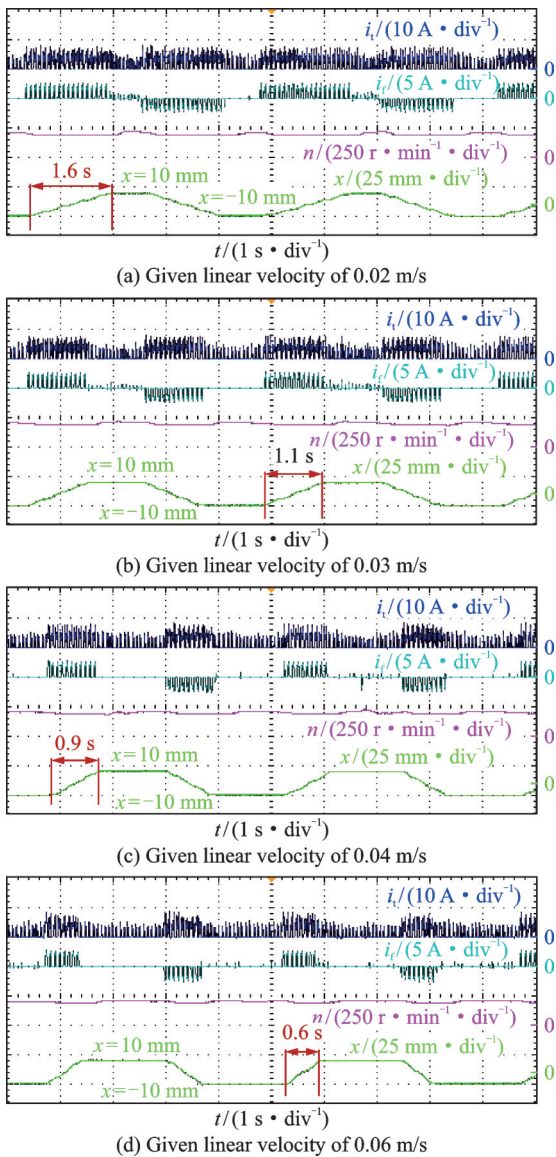


Fig.15 Reciprocating motion experiments of linear velocity control

Comparing Fig.13 and Fig.15 with Fig.10, we observed that the original control method can only determine the axial displacement, but the linear velocity cannot be adjusted. The linear velocity control

method proposed can regulate the axial displacement and positioning time simultaneously, while the rotor rotated at the given speed.

Table 3 shows the experimental data of linear velocity control. v_{ref} represents the given linear velocity, and v_z the average velocity of axial displacement of 20 mm. Δz represents the displacement fluctuation and Δn the speed fluctuation. The schematic diagram of axial velocity and displacement is shown in Fig.16. The axial displacement of rotor is short, and there is a process of acceleration and deceleration during axial movement. Also, the axial-velocity detection in the experiment is discrete rather than continuous. Therefore, the calculated average velocity v_z is less than v_{ref} .

Table 3 Experimental data

Experiment	$v_{ref}/$ ($m \cdot s^{-1}$)	$v_z/$ ($m \cdot s^{-1}$)	$\Delta z/\%$	$\Delta n/\%$
Axial positioning	0.04	0.022	2	2
	0.06	0.033		
	0.08	0.050		
	0.10	0.070		
Reciprocating motion	0.02	0.013	2	2
	0.03	0.018		
	0.04	0.022		
	0.06	0.033		

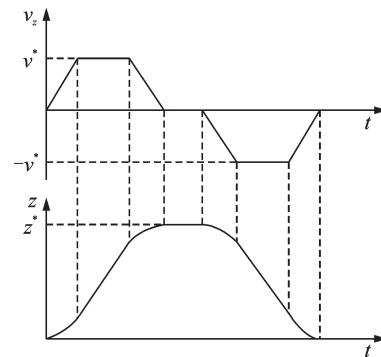


Fig.16 Schematic diagram of axial velocity and displacement

5 Conclusions

Based on an LRSRM with two radial windings, the paper analyzes the motion principle of LRSRM and proposes a new linear velocity control method. Conclusions are drawn as follows:

(1) In the field of LRM control, accurate and independent active control of the two-DoF motion is important. The linear velocity control method proposed can not only control rotary motion and axial positioning of the rotor, but also further control the linear velocity and regulate the axial positioning time of the rotor during the rotation process.

(2) Through the linear position/velocity observer, coordinated control of axial displacement and linear velocity is realized. The response speed of axial motion can be improved. Furthermore, the application of LRSRM is broaden because the axial positioning is adjustable and suitable for different applications such as 3-D printer, screwing machine, vacuum-assisted device and so on.

(3) The steady-state and dynamic simulations are carried out. When rotating at the given speed, the rotor can run to a specified axial position at a given axial velocity. On this basis, experiments are performed on the 6/4 pole LRSRM experimental platform to prove the effectiveness of the control method. The time taken to move axially from -10 mm to 10 mm is 0.9, 0.6, 0.4, and 0.3 s by controlling linear velocity, while the axial positioning time is 1.5 s with the original control method. In reciprocating motion, the positioning time is 1.6, 1.1, 0.9, and 0.6 s with the proposed linear velocity control method while 0.8 s with the original control method.

References

- [1] XU L, LIN M Y, FU X H, et al. Analysis of a double stator linear rotary permanent magnet motor with orthogonally arrayed permanent magnets[J]. *IEEE Transactions on Magnetics*, 2016, 52(7): 1-4.
- [2] BOLOGNESI P, BRUNO O, TAPONNECCO L. Dual-function wheel drives using rotary-linear actuators in electric and hybrid vehicles[C]//*Proceedings of the 2009 35th Annual Conference of IEEE Industrial Electronics*. Porto: IEEE, 2009.
- [3] BOLOGNESI P, PAPINI F. FEM modeling and analysis of a novel rotary-linear isotropic brushless machine[C]//*Proceedings of the XIX International Conference on Electrical Machines—ICEM 2010*. Rome: IEEE, 2010.
- [4] XIE Lujia, SI Jikai, HU Yihua, et al. Overview of 2-degree-of-freedom rotary-linear motors focusing on coupling effect[J]. *IEEE Transactions on Magnetics*, 2019, 55(4): 1-11.
- [5] ZHAO S W, CHEUNG N C, GAN W, et al. A self-tuning regulator for the high-precision position control of a linear switched reluctance motor[J]. *IEEE Transactions on Industrial Electronics*, 2007, 54(5): 2425-2434.
- [6] TURNER A, RAMSAY K, CLARK R, et al. Direct-drive rotary-linear electromechanical actuation system for control of gearshifts in automated transmissions[C]//*Proceedings of the 2007 IEEE Vehicle Power and Propulsion Conference*. Arlington: IEEE, 2007.
- [7] WANG Q J, XIA K. The motion control algorithm based on quaternion rotation for a permanent magnet spherical stepper motor[C]//*Proceedings of the 2006 CES/IEEE 5th International Power Electronics and Motion Control Conference*. Shanghai: IEEE, 2006.
- [8] SATO Y. Development of a 2-degree-of-freedom rotational/linear switched reluctance motor[J]. *IEEE Transactions on Magnetics*, 2007, 43(6): 2564-2566.
- [9] SATO Y, MURAKAMI K, TSUBOI Y. Sensorless torque and thrust estimation of a rotational/linear two degrees-of-freedom switched reluctance motor[J]. *IEEE Transactions on Magnetics*, 2016, 52(7): 1-4.
- [10] BENÏIA I, RUBA M, SZABÓ L. On the control of a rotary-linear switched reluctance motor[C]//*Proceedings of the 2011 5th International Symposium on Computational Intelligence and Intelligent Informatics (ISCIII)*. Floriana: IEEE, 2011.
- [11] PAN J F, ZOU Y, CHEUNG N C. Performance analysis and decoupling control of an integrated rotary—Linear machine with coupled magnetic paths[J]. *IEEE Transactions on Magnetics*, 2014, 50(2): 761-764.
- [12] PAN J, MENG F, CAO G. Decoupled control for integrated rotary-linear switched reluctance motor[J]. *IET Electric Power Applications*, 2014, 8(5): 199-208.
- [13] LI S Y, CHENG K W E, CHEUNG N, et al. Design and control of a decoupled rotary-linear switched reluctance motor[J]. *IEEE Transactions on Energy Conversion*, 2018, 33(3): 1363-1371.
- [14] ZOU Y, CHENG K W E, HU J F, et al. A new decoupled rotlin motor with fuzzy sliding mode control[J]. *IEEE Transactions on Magnetics*, 2018, 54(11): 1-5.

- [15] HE Zhouhui, CAO Xin, CHEH Huateng, et al. Speed and axial position control for a linear-rotary switched reluctance motor with two radial windings [J]. IEEE Transactions on Industrial Electronics, 2023, 70(9): 8757-8767.

Acknowledgements This work was supported by the National Natural Science Foundations of China (Nos.51877107, 52377056).

Authors Miss. MENG Xuying graduated from Nanjing University of Aeronautics and Astronautics in 2022, majoring in electrical engineering. She is currently studying for a master's degree in electrical engineering from Nanjing University of Aeronautics and Astronautics, China. Her current research focuses on linear-rotary switched reluctance motors. Prof. CAO Xin received the B.S., M.S. and Ph.D. degrees in electrical engineering from Nanjing University of Aeronautics and Astronautics, Nanjing, China, in 2003, 2006, and 2010, respectively. Since 2011, he has been in Nanjing Uni-

versity of Aeronautics and Astronautics, where he is currently a professor at the Department of Electrical Engineering. From June 2011 to September 2012, he was a research associate in the Department of Aeronautical and Automotive Engineering, Loughborough, University, Loughborough, U. K. His current research interests include virtual synchronous machines, multi-degree-of-freedom motors and high speed machines.

Author contributions Miss. MENG Xuying and Prof. CAO Xin designed the study, compiled the models, conducted the analysis, interpreted the results and wrote the manuscript. Mr. SHI Ruijie contributed to data and components for the model. Mr. HE Zhouhui, Dr. DENG Xu and Prof. DENG Zhiqian contributed to the discussion and background of the study. All authors commented on the manuscript draft and approved the submission.

Competing interests The authors declare no competing interests.

(Production Editor: SUN Jing)

直线旋转开关磁阻电机的轴向速度控制与快速轴向定位

孟徐颖¹, 曹鑫¹, 石瑞杰¹, 何洲辉¹, 邓旭², 邓智泉¹

(1. 南京航空航天大学自动化学院, 南京 210016, 中国;

2. 纽卡斯尔大学工程学院, 纽卡斯尔泰恩河畔 NE1 7RU, 英国)

摘要: 目前直线旋转开关磁阻电机 (Linear-rotary switched reluctance motor, LRSRM) 只可实现轴向定位控制, 两自由度运动方式较为单一。为提高 LRSRM 轴向控制性能, 本文提出了一种轴向速度控制方法, 通过线性位置/速度观测器协调控制转子的轴向位移和轴向速度, 由转矩与轴向力的数学模型解算出转矩及轴向力绕组的给定电流, 再将其分配到对应的绕组导通区间, 分别进行电流滞环控制。该方法可以有效调节转子在旋转过程中的轴向定位速度。仿真和实验验证了所提方法的控制效果。

关键词: 多自由度电机; 直线旋转开关磁阻电机; 轴向速度控制; 快速轴向定位